

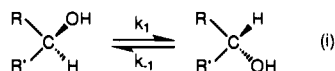
# Epimerization of Secondary Alcohols by New Homogeneous, Low Oxidation State Metal Catalysts: Carbon-Hydrogen Bond Activation in Rhenium Alkoxide Complexes ( $\eta^5\text{-C}_5\text{R}_5$ )Re(NO)(PPh<sub>3</sub>)(OCHR'R')

Isabel Saura-Llamas and J. A. Gladysz\*

Contribution from the Department of Chemistry, University of Utah, Salt Lake City, Utah 84112. Received September 6, 1991

**Abstract:** Diastereomerically pure secondary alcohols epimerize to mixtures of diastereomers in C<sub>6</sub>H<sub>5</sub>R at 65–90 °C in the presence of 10 mol % ( $\eta^5\text{-C}_5\text{R}_5$ )Re(NO)(PPh<sub>3</sub>)(OCH<sub>3</sub>) (**1**; R = H, Me). The methoxide ligand of **1** first exchanges with the alcohol substrate to give alkoxide complexes ( $\eta^5\text{-C}_5\text{R}_5$ )Re(NO)(PPh<sub>3</sub>)(OCHR'R') (**2**). Authentic samples of diastereomerically and enantiomerically pure **2** are prepared, where OCHR'R' is derived from (+)- and (-)-, *exo*- and *endo*-borneol. NMR data show that epimerization occurs first at rhenium (ca. 35 °C) and then at carbon (ca. 65 °C). Substitution reactions and rate experiments show that PPh<sub>3</sub> initially dissociates from **2** with anchimeric assistance by alkoxide oxygen lone pairs. An intermediate with a trigonal-planar rhenium, which can either return to **2** (with epimerization at rhenium) or undergo  $\beta$ -hydride elimination to a ketone hydride complex (leading to epimerization at carbon), is proposed. Accordingly, rates of epimerization at carbon (but not rhenium) are strongly inhibited by added PPh<sub>3</sub>, and show a significant  $k_H/k_D$ .

Secondary alcohols are the most common heteroatom-substituted stereocenters in organic molecules. Many stereoselective syntheses have been reported, and efficient *stoichiometric* methods for *inverting* configuration have been developed.<sup>1</sup> However, the need to *randomize* or *equilibrate* configuration, although somewhat less aesthetic from a design standpoint, can also arise (eq i). For example, both classical chemical and modern enzymatic<sup>2</sup>



R, R' contain additional stereocenters: epimerization (interconversion of diastereomers)

R, R' contain no additional stereocenters: racemization (interconversion of enantiomers)

resolutions frequently produce unwanted enantiomers as byproducts. These pose a waste disposal problem unless recycled. Also, diastereomeric equilibria can be sufficiently biased that *epimerization* constitutes a viable synthetic strategy. Finally, epimerization reactions facilitate the determination of equilibrium constants.

Accordingly, considerable attention has been directed at the development of methods for the *catalytic* epimerization (or racemization) of secondary alcohols.<sup>3-4</sup> Importantly, any change of configuration at a tetrahedral carbon commonly requires bond breaking. Thus, such transformations must belong to one of three mechanistic categories: carbon-oxygen bond activation processes, carbon-hydrogen bond activation processes, and carbon-carbon bond activation processes.

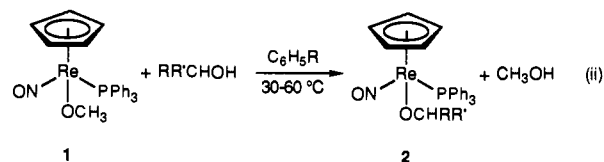
In this paper, we report that rhenium(I) methoxide complexes of the formula ( $\eta^5\text{-C}_5\text{R}_5$ )Re(NO)(PPh<sub>3</sub>)(OCH<sub>3</sub>) are active catalysts for the epimerization of secondary alcohols in aromatic hydrocarbons at 65–90 °C. To our knowledge, these constitute the first well-defined homogeneous epimerization catalysts in-

volving transition metals in low oxidation states. We also describe a variety of mechanistic experiments that offer a detailed view of the reaction coordinate—an undertaking facilitated by the *chirality* of the catalysts. A portion of this study has been communicated.<sup>5</sup>

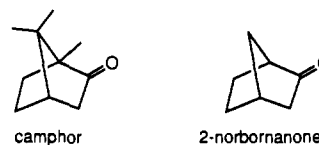
## Results

**1. Scope of Reaction.** The diastereomerically pure alcohols shown in Table I were dissolved in deuterated benzene or toluene. Then 10 mol % of the racemic methoxide complex ( $\eta^5\text{-C}_5\text{H}_5$ )Re(NO)(PPh<sub>3</sub>)(OCH<sub>3</sub>) (**1**)<sup>6</sup> was added. The samples were kept at 65–90 °C, and monitored by <sup>1</sup>H NMR spectroscopy. In all cases, the alcohols epimerized to mixtures of diastereomers, as summarized in Table I. Ratios were determined by integration of the *CHOH* resonances, verified by replicate experiments and other analyses (below), and normalized to 100. Error limits on each integer are estimated as  $\pm 2$ .

The <sup>1</sup>H NMR spectra of the reaction mixtures further revealed that the methoxide ligand of **1** initially exchanged with the alcohol substrate to give secondary alkoxide complexes ( $\eta^5\text{-C}_5\text{H}_5$ )Re(NO)(PPh<sub>3</sub>)(OCHR'R') (**2**), as shown in eq ii. These metathesis products were also evident in <sup>31</sup>P NMR spectra, and some were independently prepared as described below.



Separate reactions were conducted in the presence of GC standards. The *endo/exo*-borneol and -norborneol ratios were identical to those found above, within experimental error. Also, small amounts of the corresponding ketones were detected: camphor (5%) from *exo*-borneol; 2-norbornanone (5%) from



(5) Saura-Llamas, I.; Garner, C. M.; Gladysz, J. A. *Organometallics* 1991, 10, 2533.

(6) (a) Buhro, W. E.; Georgiou, S.; Fernández, J. M.; Patton, A. T.; Strouse, C. E.; Gladysz, J. A. *Organometallics* 1986, 5, 956. (b) Agbossou, S. K.; Smith, W. W.; Gladysz, J. A. *Chem. Ber.* 1990, 123, 1293.

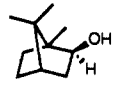
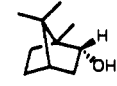

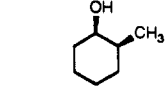
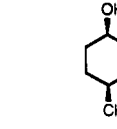
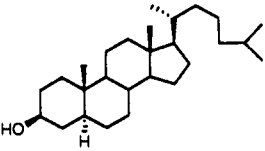
(1) (a) Mitsunobu, O. *Synthesis* 1981, 1. (b) Torisawa, Y.; Okabe, H.; Ikegami, S. *Chem. Lett.* 1984, 1555 and references therein. (c) Martin, S. F.; Dodge, J. A. *Tetrahedron Lett.* 1991, 32, 3017 and references therein.

(2) (a) Klivanov, A. M. *Acc. Chem. Res.* 1990, 23, 114. (b) Burgess, K.; Jennings, L. D. *J. Am. Chem. Soc.* 1991, 113, 6129.

(3) (a) Feghouli, G.; Vanderesse, R.; Fort, Y.; Caubère, P. *Tetrahedron Lett.* 1988, 29, 1383. (b) Vanderesse, R.; Feghouli, G.; Fort, Y.; Caubère, P. *J. Org. Chem.* 1990, 55, 5916. (c) Nugent, W. A.; Zubyk, R. M. *Inorg. Chem.* 1986, 25, 4604. (d) Choudary, B. M. *Polyhedron* 1986, 5, 2117.

(4) (a) Eliel, E. L.; Ro, R. S. *J. Am. Chem. Soc.* 1957, 79, 5992. (b) Eliel, E. L.; Rerick, M. N. *Ibid.* 1960, 82, 1367. (c) Eliel, E. L.; Schroeter, S. H. *Ibid.* 1965, 87, 5031. (d) Eliel, E. L.; Schroeter, S. H.; Brett, T. J.; Biros, F. J.; Richer, J.-C. *Ibid.* 1966, 88, 3327. (e) Wilcox, C. F., Jr.; Sexton, M.; Wilcox, M. F. *J. Org. Chem.* 1963, 28, 1079.

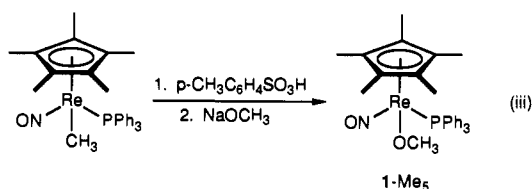
**Table I.** Data on the Epimerization of Secondary Alcohols by 10 mol % ( $\eta^5\text{-C}_5\text{R}_5$ )Re(NO)(PPh<sub>3</sub>)(OCH<sub>3</sub>)

starting alcohol	catalyst	temp (°C)	time (h)	reactant/product	$k_1 \times 10^5$ (s <sup>-1</sup> )	$k_{-1} \times 10^5$ (s <sup>-1</sup> )
 (±)- <i>exo</i> -borneol <sup>a</sup>	1	65	48	32/68 <sup>c</sup>	2.7 ± 0.2	1.3 ± 0.2
	1	65		32/68 <sup>c</sup>	2.2 ± 0.2	1.1 ± 0.2
	1-Me <sub>5</sub>	65	48	30/70 <sup>c</sup>	14 ± 1	5 ± 1
 (±)- <i>endo</i> -borneol <sup>a</sup>	1	65	48	68/32 <sup>d</sup>	1.2 ± 0.1	2.5 ± 0.1
	1	71	180	24/76 <sup>d</sup>	0.52 ± 0.01	0.16 ± 0.01
 (±)- <i>endo</i> -norborneol <sup>a</sup>	1	71		24/76 <sup>d</sup>	0.63 ± 0.01	0.20 ± 0.01
	1-Me <sub>5</sub>	71	162	18/82 <sup>d</sup>	1.03 ± 0.04	0.22 ± 0.04
	1	80	80	30/70 <sup>e</sup>	0.51 ± 0.03	0.21 ± 0.03
 (±)- <i>cis</i> -2-methylcyclohexanol <sup>a</sup>	1	80		28/72 <sup>e</sup>	0.51 ± 0.03	0.20 ± 0.03
	1	80		28/72 <sup>e</sup>	0.51 ± 0.03	0.20 ± 0.03
	1-Me <sub>5</sub>	80	52	23/77 <sup>e</sup>	0.91 ± 0.04	0.27 ± 0.04
 <i>cis</i> -4-methylcyclohexanol <sup>b</sup>	1	91	40	28/72 <sup>e</sup>	1.5 ± 0.1	0.6 ± 0.1
	1	91		30/70 <sup>e</sup>	1.1 ± 0.1	0.5 ± 0.1
	1-Me <sub>5</sub>	93	14	30/70 <sup>e</sup>	3.9 ± 0.1	1.7 ± 0.1
 (+)- <i>cis</i> -α-cholestanol <sup>a</sup>	1	80	48	28/72 <sup>f</sup>	1.2 ± 0.1	0.5 ± 0.1
	1	80		28/72 <sup>f</sup>	1.0 ± 0.1	0.4 ± 0.1
	1-Me <sub>5</sub>	80	48	30/70 <sup>f</sup>	1.9 ± 0.1	0.8 ± 0.1

<sup>a</sup>In C<sub>6</sub>D<sub>6</sub>. <sup>b</sup>In C<sub>6</sub>D<sub>5</sub>CD<sub>3</sub>. <sup>c</sup>*exo*/*endo*. <sup>d</sup>*endo*/*exo*. <sup>e</sup>*cis*/*trans*. <sup>f</sup>α/β.

*endo*-norborneol; 2-methylcyclohexanone (3–5%) from 2-methylcyclohexanol. Ketone byproducts have also been observed with other epimerization catalysts.<sup>3,4c</sup> Good mass balance was achieved in all cases. For example, the epimerization of *exo*-borneol gave *exo*-borneol (33%), *endo*-borneol (62%), and camphor (5%).

Related, potentially more reactive catalysts were sought. Thus, the *pentamethylcyclopentadienyl* complex ( $\eta^5\text{-C}_5\text{Me}_5$ )Re(NO)(PPh<sub>3</sub>)(OCH<sub>3</sub>) (1-Me<sub>5</sub>) was prepared from the methyl complex ( $\eta^5\text{-C}_5\text{Me}_5$ )Re(NO)(PPh<sub>3</sub>)(CH<sub>3</sub>)<sup>7</sup> as shown in eq iii.



This route is analogous to one described earlier for 1.<sup>6a</sup> Complex 1-Me<sub>5</sub> was characterized by microanalysis, and IR and NMR (<sup>1</sup>H, <sup>13</sup>C, <sup>31</sup>P) spectroscopy, as summarized in the Experimental Section. The properties resembled those previously reported for 1 and other alkoxide complexes.<sup>5,8</sup>

Complex 1-Me<sub>5</sub> also catalyzed the epimerization of secondary alcohols, as shown in Table I. Rates of the preceding reactions were measured by <sup>1</sup>H NMR spectroscopy. The approach to apparent equilibrium was first order, as indicated by linear plots of ln ([C]<sub>equil</sub> - [C]) vs time.<sup>9</sup> The final alcohol ratios in Table

I represent values that remained constant (within the ±2 error limit) over a 24-h period. These data gave the forward and reverse rate constants,  $k_1$  and  $k_{-1}$ , shown in Table I.

Several trends were evident in the rate data. First, the  $k_1$  values for 1-Me<sub>5</sub> were 2–4 times greater than those for 1. Second, the  $k_1/k_{-1}$  values for *exo*-borneol closely matched the  $k_{-1}/k_1$  values for *endo*-borneol. Third, the sterically more congested alcohols underwent epimerization more rapidly. Analogous rate trends are apparent with other catalysts, although exceptions are known.<sup>4c</sup>

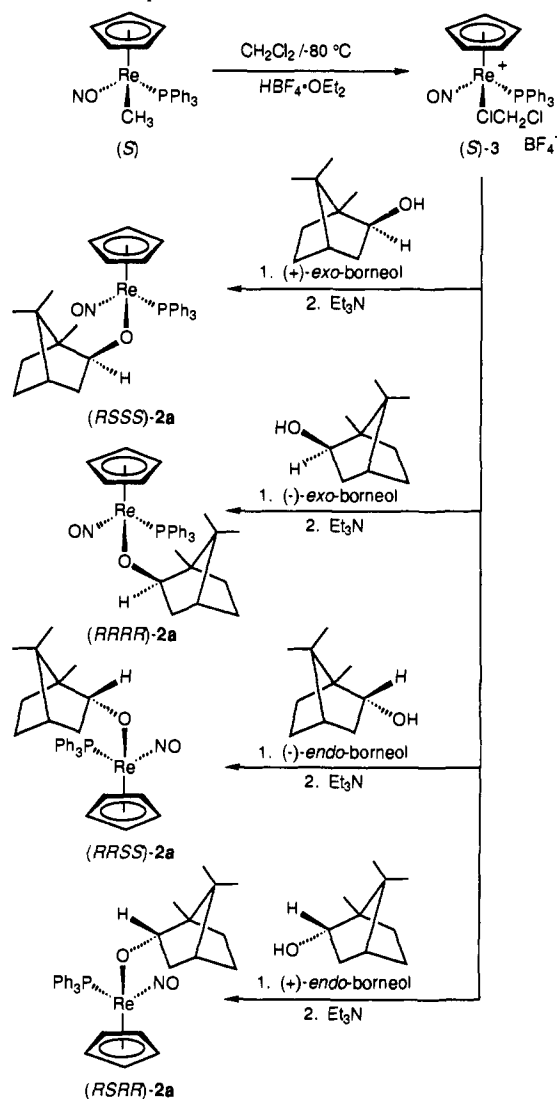
The final alcohol ratios obtained with the more active catalyst 1-Me<sub>5</sub> were in some cases slightly greater than those obtained with 1. Thus, true thermodynamic equilibrium may not be reached under all conditions in Table I. Additional experiments were conducted to probe this point. First, the epimerization of *exo*-borneol was repeated with 5, 15, and 20 mol % of 1. After 48 h, the *exo*/*endo* ratios were 49/51, 33/67, and 32/68, respectively. After 72 h, the ratios were 47/53, 32/68, and 30/70. The epimerization with 10 mol % of 1 was repeated at 80 °C. After 48 and 72 h, the *exo*/*endo* ratios were 33/67 and 31/69. The <sup>31</sup>P NMR spectra of these samples showed the presence of PPh<sub>3</sub> (ca. 2%), suggestive of some catalyst degradation. Some possible implications are analyzed below.

**2. Definition of Configurational Processes.** In order to help probe the mechanisms of the preceding epimerizations, diastereomerically and enantiomerically pure samples of 2 were sought. In particular, complexes with a third, "spectator" stereocenter would allow the simultaneous monitoring of configuration at both rhenium and carbon.

(7) Patton, A. T.; Strouse, C. E.; Knobler, C. B.; Gladysz, J. A. *J. Am. Chem. Soc.* **1983**, *105*, 5804.

(8) (a) Garner, C. M.; Quirós Méndez, N.; Kowalczyk, J. J.; Fernández, J. M.; Emerson, K.; Larsen, R. D.; Gladysz, J. A. *J. Am. Chem. Soc.* **1990**, *112*, 5146. (b) Dalton, D. M.; Fernández, J. M.; Emerson, K.; Larsen, R. D.; Arif, A. M.; Gladysz, J. A. *Ibid.* **1990**, *112*, 9198.

(9) (a) Capellos, C.; Bielski, B. H. J. *Kinetic Systems*; Wiley: New York, 1972; Chapter 8. (b) The linearity of ln ([C]<sub>equil</sub> - [C]) vs time plots is sensitive to the value of [C]<sub>equil</sub> (or  $K_{eq}$ ), and provide a check of these data. Thus, normalized equilibrium ratios were adjusted by up to ±2 (the experimental error) to optimize linearity. (c) Error limits on rate constants represent standard deviations on the slopes of ln [C] or ln ([C]<sub>equil</sub> - [C]) vs time plots.

**Scheme I.** Syntheses of Authentic Samples of Diastereomerically Pure Alkoxide Complexes

Toward this objective, the optically active methyl complex  $(+)$ - $(S)$ - $(\eta^5\text{-C}_5\text{H}_5)\text{Re}(\text{NO})(\text{PPh}_3)(\text{CH}_3)^{10}$  was treated with  $\text{HBF}_4 \cdot \text{OEt}_2$  in  $\text{CH}_2\text{Cl}_2$  at  $-80^\circ\text{C}$  to generate the dichloromethane complex  $(S)\text{-}[(\eta^5\text{-C}_5\text{H}_5)\text{Re}(\text{NO})(\text{PPh}_3)(\text{CICH}_2\text{Cl})]^+\text{BF}_4^-$  ( $(S)\text{-}3$ ; Scheme I).<sup>11</sup> This substitution-labile compound has previously been shown to react with a variety of Lewis bases with retention of configuration at rhenium.<sup>12</sup> Also, racemic **3** reacts with primary and secondary alcohols to give the corresponding cationic alcohol complexes.<sup>6b,8b</sup> These are in turn easily deprotonated to alkoxide complexes.

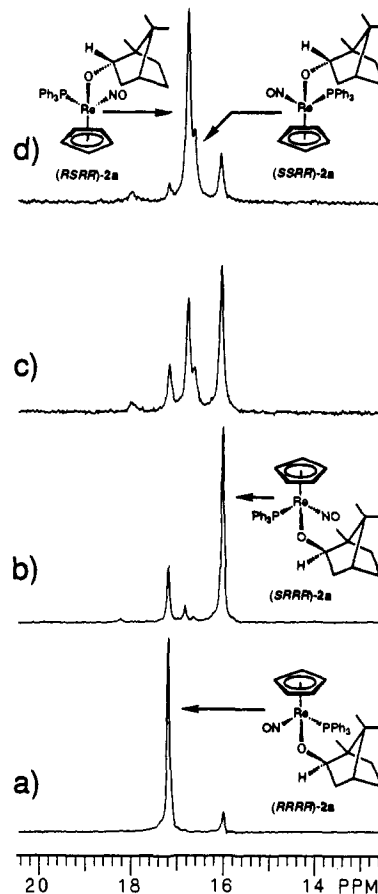
Thus,  $(S)\text{-}3$  was treated with authentic samples of  $(+)$ -exo-borneol,  $(-)$ -exo-borneol,  $(-)$ -endo-borneol, and  $(+)$ -endo-borneol. Subsequent addition of  $\text{Et}_3\text{N}$ , and workup, gave the four diastereomeric alkoxide complexes  $(RSSS)\text{-}2a$ ,  $(RRRR)\text{-}2a$ ,  $(RRSS)\text{-}2a$ , and  $(RSRR)\text{-}2a$  shown in Scheme I. Each was presumed to form with retention at rhenium, and was diastereomerically pure (within detection limits) provided that careful attention was given to workup temperature. In all cases, the absolute configuration at rhenium is specified first,<sup>8</sup> and that of the alkoxide carbon is given second.

Complexes **2a** were highly lipophilic powders that were difficult to purify and (in some cases) separate from traces of alcohols.

(10) Merrifield, J. H.; Strouse, C. E.; Gladysz, J. A. *Organometallics* **1982**, *1*, 1204.

(11) Fernández, J. M.; Gladysz, J. A. *Organometallics* **1989**, *8*, 207.

(12) These processes are *associative* and are mechanistically distinct from the  $\text{PPh}_3$  substitution reactions described in this paper. Garner, C. M.; Liu, Y. Unpublished data, University of Utah.



**Figure 1.** Epimerization of  $(RRRR)\text{-}2a$ : (a)  $^{31}\text{P}\{^1\text{H}\}$  NMR spectrum of starting material at  $35^\circ\text{C}$ ; (b) spectrum after  $9$  h at  $35^\circ\text{C}$ ; (c) and (d) spectra after  $0.6$  and  $10$  h at  $65^\circ\text{C}$ .

The extreme reactivity of the  $\text{Re}\text{-O}$  alkoxide linkage toward electrophiles has been previously documented.<sup>8</sup> Reasonable microanalyses were achieved for  $(RRRR)\text{-}2a$  and  $(RSRR)\text{-}2a$ , but at some sacrifice in yield. Spectroscopic properties are summarized in the Experimental Section. Importantly, all complexes gave distinct  $\text{PPh}_3$   $^{31}\text{P}$  NMR chemical shifts, which were slightly temperature dependent.

Next, the epimerization of  $(RRRR)\text{-}2a$  was monitored by  $^{31}\text{P}$  NMR spectroscopy. Representative spectra are shown in Figure 1. A diastereomer with a chemical shift ( $16.0$  ppm) corresponding to that of  $(RSSS)\text{-}2a$  (Scheme I) formed first. However, this would require the simultaneous inversion of all three carbon stereocenters—including two bridgehead positions! Any such process is clearly unreasonable. Hence, the new resonance was assigned to the *enantiomer*  $(SRRR)\text{-}2a$ , derived from epimerization at rhenium.

At higher temperatures, resonances appeared at  $16.8$  ppm (major) and  $16.6$  ppm (minor). The former corresponds to that of  $(RSRR)\text{-}2a$ , an authentic sample of which was prepared in Scheme I. The latter corresponds to  $(SSRR)\text{-}2a$ , the *enantiomer* of which was prepared in Scheme I. These diastereomers can only be derived by *carbon* epimerization. Thus, the carbon stereocenter of **2a** epimerizes more slowly than the rhenium stereocenter.

**3. Phosphine Substitution.** Having defined the operation of two distinct epimerization processes, we sought detailed mechanistic data on each. Previously,  $\text{PPh}_3$  ligand dissociation has been shown to play a key role in the epimerization of diastereomeric amide complexes  $(\eta^5\text{-C}_5\text{H}_5)\text{Re}(\text{NO})(\text{PPh}_3)(\text{NHCHRR})$  at rhenium ( $40\text{--}60^\circ\text{C}$ ).<sup>13</sup> Thus,  $\text{PPh}_3$  ligand substitution reactions of **1** and **2** were studied.

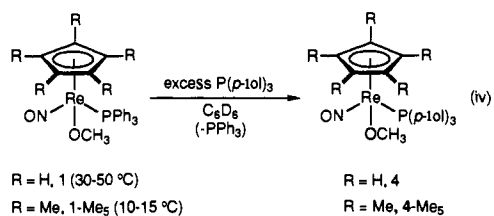
First, the methoxide complex **1** was treated with  $20$  equiv of  $\text{P}(p\text{-tol})_3$  in  $\text{C}_6\text{D}_6$ . Substitution cleanly occurred at  $30\text{--}50^\circ\text{C}$  to

(13) Dewey, M. A.; Gladysz, J. A. *Organometallics* **1990**, *9*, 1351.

**Table II.** Rates of Substitution of PPh<sub>3</sub> by Excess P(*p*-tol)<sub>3</sub>

entry	temp (°C)	P( <i>p</i> -tol) <sub>3</sub> (equiv/M)	<i>k</i> <sub>obs</sub> × 10 <sup>5</sup> (s <sup>-1</sup> )
$(\eta^5\text{-C}_5\text{H}_5)\text{Re}(\text{NO})(\text{PPh}_3)(\text{OCH}_3)$ ( <b>1</b> )			
1	32	20/0.7	2.80 ± 0.03
2	32	20/0.7	3.09 ± 0.02
3	33	20/0.7	3.14 ± 0.04
4	37	18/0.7	5.96 ± 0.03
5	41	20/0.8	9.7 ± 0.2
6	43	20/0.8	12.7 ± 0.3
7	53	20/0.8	37 ± 2
8	53	20/0.8	33 ± 2
9	53	21/0.7	29.7 ± 0.3
10	32	10/0.4	2.83 ± 0.01
$(\eta^5\text{-C}_5\text{Me}_5)\text{Re}(\text{NO})(\text{PPh}_3)(\text{OCH}_3)$ ( <b>1-Me<sub>5</sub></b> )			
11	14	20/0.7	18.4 ± 0.2
12	19	20/0.6	47.9 ± 0.9
$(RRRR)\text{-}(\eta^5\text{-C}_5\text{H}_5)\text{Re}(\text{NO})(\text{PPh}_3)(\text{exo-OC}_{10}\text{H}_{17})$ ( <b>(RRRR)-2a</b> )			
13	21	10/0.3	3.12 ± 0.04
14	21	10/0.3	3.19 ± 0.04
15	25	10/0.3	5.80 ± 0.07
16	31	11/0.4	14.1 ± 0.4
17	31	10/0.5	15.0 ± 0.3
18	32	11/0.4	17.6 ± 0.3
19	36	10/0.5	31 ± 1
20	41	10/0.3	49 ± 5
21	31	21/0.2	14.4 ± 0.2

give the new complex  $(\eta^5\text{-C}_5\text{H}_5)\text{Re}(\text{NO})(\text{P}(\textit{p}\text{-tol})_3)(\text{OCH}_3)$  (**4**), as shown in eq iv. An authentic sample of **4** was independently

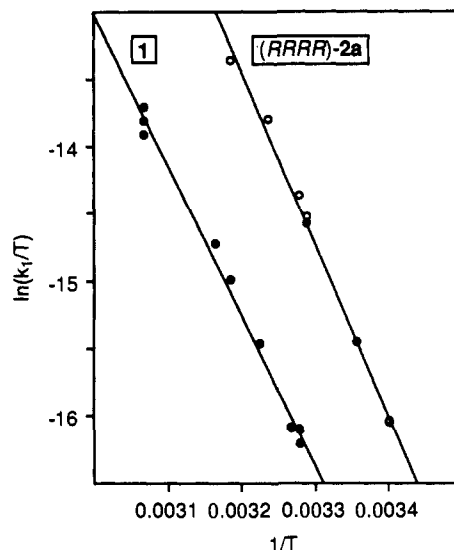


prepared from the methyl complex  $(\eta^5\text{-C}_5\text{H}_5)\text{Re}(\text{NO})(\text{P}(\textit{p}\text{-tol})_3)(\text{CH}_3)$ <sup>14</sup> by a route analogous to that in eq iii. Characterization is summarized in the Experimental Section. The <sup>31</sup>P NMR resonance of **4** was 2.8 ppm downfield of that of **1**—a shift typical of PPh<sub>3</sub>/P(*p*-tol)<sub>3</sub> analogues in this series of compounds.<sup>13,14</sup>

Rates of appearance of **4** were measured by <sup>31</sup>P NMR spectroscopy over the temperature range of 32–53 °C and through (1–4)<sub>1/2</sub> (depending upon temperature). Simple first-order rate laws were obeyed, and data are summarized in Table II (entries 1–10). The *k*<sub>obs</sub> were independent of P(*p*-tol)<sub>3</sub> concentration, as would be expected of a dissociative process. An Eyring plot (Figure 2) gave  $\Delta H^\ddagger = 22 \pm 1$  kcal/mol and  $\Delta S^\ddagger = -7 \pm 3$  eu.<sup>15</sup>

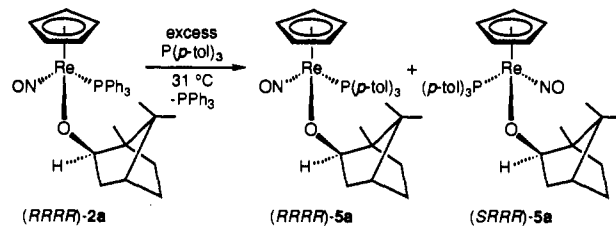
The pentamethylcyclopentadienyl complex **1-Me<sub>5</sub>** was similarly treated with P(*p*-tol)<sub>3</sub> in C<sub>6</sub>D<sub>6</sub>. A much more rapid substitution occurred to give  $(\eta^5\text{-C}_5\text{Me}_5)\text{Re}(\text{NO})(\text{P}(\textit{p}\text{-tol})_3)(\text{OCH}_3)$  (**4-Me<sub>5</sub>**), which was characterized in situ by NMR spectroscopy (<sup>31</sup>P, 14.4 (s) ppm; <sup>1</sup>H,  $\delta$  4.34 (s, OCH<sub>3</sub>), 2.03 (s, 5 CCH<sub>3</sub>), 1.55 (s, 3 CCH<sub>3</sub>)). Rates of appearance of **4-Me<sub>5</sub>** were measured at 14 and 19 °C (Table II, entries 11–12). The rates of appearance of **4** at 14 and 19 °C were extrapolated as  $0.29 \times 10^{-5}$  and  $0.57 \times 10^{-5}$  s<sup>-1</sup> from the Eyring plot. Thus, substitution of the PPh<sub>3</sub> ligand in **1-Me<sub>5</sub>** is 60–80 times faster than in **1**.

Next, the alkoxide complex **(RRRR)-2a**—the starting material for Figure 1—was similarly treated with P(*p*-tol)<sub>3</sub>, as shown in Scheme II. Importantly, two diastereomeric substitution products  $(\eta^5\text{-C}_5\text{H}_5)\text{Re}(\text{NO})(\text{P}(\textit{p}\text{-tol})_3)(\text{OC}_{10}\text{H}_{17})$  (**5a**) formed. These were assigned as **(RRRR)-5a** and **(SRRR)-5a** on the basis of their <sup>31</sup>P NMR chemical shifts (14.2 and 13.2 ppm), and precedent with



**Figure 2.** Eyring plots for reactions of alkoxide complexes **1** and **(RRRR)-2a** with P(*p*-tol)<sub>3</sub>.

**Scheme II.** Reaction of **(RRRR)-2a** and P(*p*-tol)<sub>3</sub>



10 equiv P( <i>p</i> -tol) <sub>3</sub>			20 equiv P( <i>p</i> -tol) <sub>3</sub>		
time (min)	product ratio	conversion (%)	time (min)	product ratio	conversion (%)
6.7	63 : 37	20	6.7	62 : 38	20
93.5	60 : 40	65	90.2	60 : 40	62
166.9	58 : 44	81	172.0	56 : 44	80
277.0	50 : 50	90	280.5	50 : 50	90
350.4	46 : 54	93	345.6	47 : 53	94
497.2	41 : 59	95			
600.6	37 : 63	96			

The above data are abstracted from rate experiments (entries 16, 21 in Table II).

analogous amido complexes.<sup>13</sup> No independent epimerization of the reactant **(RRRR)-2a** occurred under the substitution conditions. However, the products **(RRRR)-5a** and **(SRRR)-5a** did interconvert. The *RRRR/SRRR* ratio was 63–62/37–38 at 20% conversion (31 °C), but 37/63 at 96% conversion. Thus, the kinetic diastereoselectivity differs from the thermodynamic diastereoselectivity. No carbon epimerization to give the endo diastereomers **(RSRR)-5a** or **(SSRR)-5a** was detected.

Rates of appearance of **(RRRR)-** and **(SRRR)-5a** were measured at 21–41 °C as described for **4** (Table II, entries 13–21). Importantly, the *k*<sub>obs</sub> and product ratios were both independent of P(*p*-tol)<sub>3</sub> concentration. The *k*<sub>obs</sub> were also approximately five times greater than those of **4**. An Eyring plot (Figure 2) gave  $\Delta H^\ddagger = 26 \pm 2$  kcal/mol and  $\Delta S^\ddagger = 8 \pm 6$  eu.

**4. Rates of Epimerization at Rhenium and Carbon.** We sought to compare the preceding substitution rates to epimerization rates. Thus, rates of conversion of **(RRRR)-2a** to the rhenium epimerization product **(SRRR)-2a** were measured in C<sub>6</sub>D<sub>6</sub> at 30–41 °C (Table III, entries 1–8). The approach to equilibrium was first order and independent of added PPh<sub>3</sub>. Rate constants were calculated as described above.<sup>9</sup> Significantly, at 31–36 °C the *k*<sub>1</sub> values were 36–40% of the corresponding *k*<sub>obs</sub> for P(*p*-tol)<sub>3</sub> substitution. As is analyzed below, this result is intuitively

(14) Dewey, M. A., Ph.D. Thesis, University of Utah, Salt Lake City, UT, 1991.

(15) Standard deviations for  $\Delta H^\ddagger$  and  $\Delta S^\ddagger$  values were estimated according to Wiberg, K. B. *Physical Organic Chemistry*; Wiley: New York, 1964; pp 378–379.

**Table III.** Summary of Alkoxide Complex Epimerization Rates

entry	temp °C	final ratio	PPh <sub>3</sub> (equiv/M)	$k_1 \times 10^5$ (s <sup>-1</sup> )	$k_{-1} \times 10^5$ (s <sup>-1</sup> )
<b>((RRRR)-(<math>\eta^5</math>-C<sub>5</sub>H<sub>5</sub>)Re(NO)(PPh<sub>3</sub>)(<i>exo</i>-OC<sub>10</sub>H<sub>17</sub>)) ((RRRR)-2a)</b>					
1	30	23/77 <sup>a</sup>		5.3 ± 0.1	1.6 ± 0.1
2	31	24/76		5.5 ± 0.1	1.7 ± 0.1
3	31	24/76		5.5 ± 0.1	1.7 ± 0.1
4	33	21/79		6.7 ± 0.1	1.8 ± 0.1
5	36	23/77		12.4 ± 0.2	3.7 ± 0.2
6	38	22/78		14.6 ± 0.2	4.1 ± 0.2
7	43	23/77		31.9 ± 0.7	9.5 ± 0.7
8	31	25/75	10/0.4	5.0 ± 0.1	1.6 ± 0.1
<b>((RSSS)-(<math>\eta^5</math>-C<sub>5</sub>H<sub>5</sub>)Re(NO)(PPh<sub>3</sub>)(<i>exo</i>-OC<sub>10</sub>H<sub>17</sub>)) ((RSSS)-2a)</b>					
9	31	79/21 <sup>b</sup>		1.4 ± 0.1	5.2 ± 0.1
<b>((RRRR)-(<math>\eta^5</math>-C<sub>5</sub>H<sub>5</sub>)Re(NO)(PPh<sub>3</sub>)(<i>exo</i>-OC<sub>10</sub>H<sub>16</sub>D)) ((RRRR)-2a-d<sub>1</sub>)</b>					
10	31	20/80 <sup>a</sup>		5.7 ± 0.1	1.4 ± 0.1
<b>((RRRR/SRRR)-(<math>\eta^5</math>-C<sub>5</sub>H<sub>5</sub>)Re(NO)(PPh<sub>3</sub>)(<i>exo</i>-OC<sub>10</sub>H<sub>17</sub>)) ((RRRR/SRRR)-2a)</b>					
11	67	28/72 <sup>c</sup>		8.4 ± 0.2	3.3 ± 0.2
12	67	<i>d</i>	13/0.3	0.4 ± 0.1	0.1 ± 0.1
<b>((RRSS/SRSS)-(<math>\eta^5</math>-C<sub>5</sub>H<sub>5</sub>)Re(NO)(PPh<sub>3</sub>)(<i>endo</i>-OC<sub>10</sub>H<sub>17</sub>)) ((RRSS/SRSS)-2a)</b>					
13	67	80/20 <sup>e</sup>		3.0 ± 0.7	12.2 ± 0.7
<b>((RRRR/SRRR)-(<math>\eta^5</math>-C<sub>5</sub>H<sub>5</sub>)Re(NO)(PPh<sub>3</sub>)(<i>exo</i>-OC<sub>10</sub>H<sub>16</sub>D)) ((RRRR/SRRR)-2a-d<sub>1</sub>)</b>					
14	66	28/72 <sup>c</sup>		4.2 ± 0.2	1.6 ± 0.2

<sup>a</sup>(RRRR)/(SRRR). <sup>b</sup>(RSSS)/(SSSS). <sup>c</sup>(RRRR/SRRR)/(SRRR/SSRR). <sup>d</sup>This reaction proceeded to only ca. 15% conversion. <sup>e</sup>This sample was racemic. Thus, the ratio represents (SRRR/RRSS)/(RRRR/RSSS), and the enantiomers.

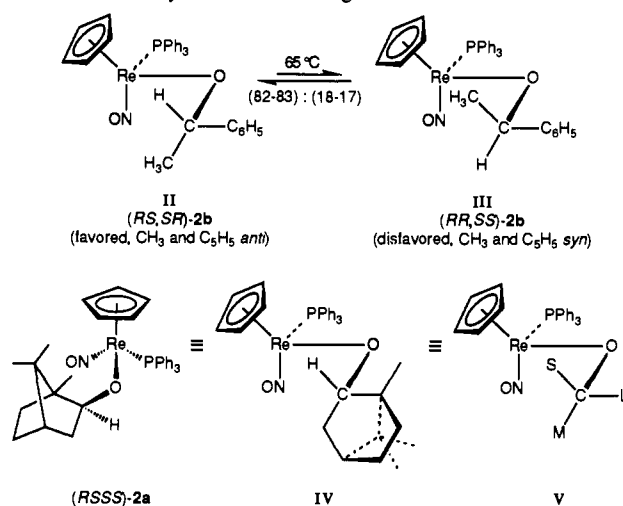
plausible: although every PPh<sub>3</sub> dissociation should lead to substitution, fewer should give inversion at rhenium.

The rate of epimerization of (RSSS)-2a to (SSSS)-2a was measured (Table III, entry 9), and gave  $k_1$  and  $k_{-1}$  values that closely matched the  $k_{-1}$  and  $k_1$  values of (RRRR)-2a. Also, a sample of *exo*-borneol-*d*<sub>1</sub> was prepared with deuterium on the carbinol carbon, and converted to the labeled alkoxide complex (RRRR)-2a-*d*<sub>1</sub>. The rate of epimerization of (RRRR)-2a-*d*<sub>1</sub> (Table III, entry 10) was virtually identical to that of (RRRR)-2a.

Next, the rate of conversion of (RRRR)-2a and (SRRR)-2a (both *exo*) to the carbon epimerization products (RSRR)-2a and (SSRR)-2a (both *endo*) was measured in C<sub>6</sub>D<sub>6</sub> at 67 °C (Table III, entry 11). Interestingly, the final *exo/endo* ratio obtained (28/72) was similar to that of the free alcohols, despite the presence of the bulky rhenium oxygen substituent. An analogous experiment was conducted in the presence of 13 equiv of PPh<sub>3</sub> (Table III, entry 12). Importantly, virtually no reaction occurred! Thus, PPh<sub>3</sub> dramatically inhibits epimerization at carbon, but not at rhenium.

The sample of (RRRR)-2a-*d*<sub>1</sub> prepared above was heated until carbon epimerization was initiated. The rate of appearance of (RSRR)-2a-*d*<sub>1</sub> and (SSRR)-2a-*d*<sub>1</sub> was then measured under conditions analogous to those used for the undeuterated analogue (Table III, entry 14). The  $k_1$  and  $k_{-1}$  values decreased by half, indicating a  $k_H/k_D$  of 2.0. Thus, there is an appreciable primary deuterium isotope effect for epimerization at carbon, but not at rhenium.

**5. Origin of Ketone Byproducts.** We sought to test whether the formation of the minor ketone byproducts noted above was reversible. Thus, camphor and the hydride complex ( $\eta^5$ -C<sub>5</sub>H<sub>5</sub>)Re(NO)(PPh<sub>3</sub>)(H) (**6**;<sup>16</sup> 1 equiv) were combined in C<sub>6</sub>D<sub>6</sub>. Concentrations were twice that of *exo*-borneol in the experiments in Table I. No reaction occurred over the course of 48 h at 65 °C, as assayed by <sup>1</sup>H and <sup>31</sup>P NMR spectroscopy. An identical reaction was conducted in the presence of a trace of the Lewis acid BF<sub>3</sub>·OEt<sub>2</sub>. The camphor remained unreacted, but **6** decomposed to a multitude of products.

**Scheme III.** Analysis of Chiral Recognition Phenomena

Next, the epimerization of *exo*-borneol was repeated in the presence of camphor-*d*<sub>1</sub> (1 equiv; 65 °C, 48 h). The recovered *exo*- and *endo*-borneol were analyzed by mass spectrometry, and the ratios of the M<sup>+</sup> - CH<sub>3</sub> (C<sub>9</sub>H<sub>15</sub>O; *m/z* 139) and M<sup>+</sup> - CH<sub>3</sub> + 1 peaks were measured (100/11 and 100/13, respectively). The theoretical ratio for natural abundance C<sub>9</sub>H<sub>15</sub>O is 100/10. Thus, little or no deuterium is incorporated.

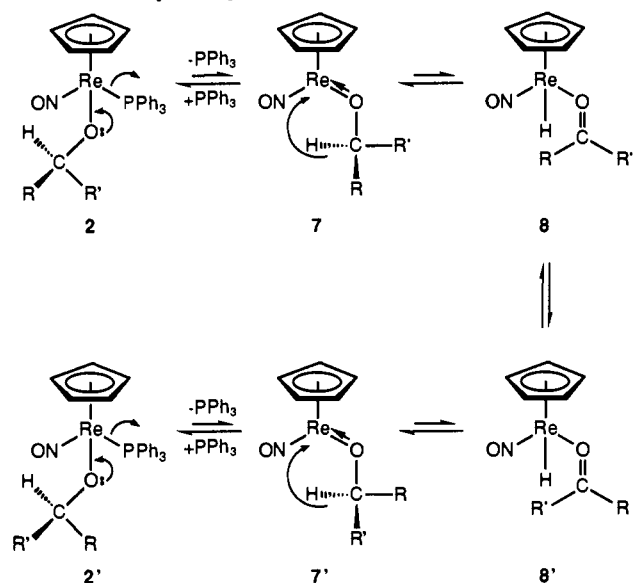
The preceding experiments indicate that ketone byproducts form irreversibly. We speculated that the methoxy ligand of the catalyst precursor **1** might be the ultimate source of an elimination-promoting base. Thus, the epimerization of *exo*-borneol was repeated with (RRRR)-2a as the catalyst. In this case, any catalyst-derived base would be bulkier and perhaps less reactive. However, GC analysis showed a comparable amount of camphor (3%), and a somewhat higher *exo/endo*-borneol ratio (23/77; 22% and 74% absolute yields).

**6. Chiral Recognition.** The epimerization of alkoxide complexes **2** provides a measure of "chiral recognition", i.e., the thermodynamic affinity of one configuration of a chiral alkoxide ligand for a given configuration of the rhenium fragment [( $\eta^5$ -C<sub>5</sub>H<sub>5</sub>)Re(NO)(PPh<sub>3</sub>)]<sup>+</sup> (**1**). We sought to define this property for the alkoxide complex ( $\eta^5$ -C<sub>5</sub>H<sub>5</sub>)Re(NO)(PPh<sub>3</sub>)(OCH(CH<sub>3</sub>)C<sub>6</sub>H<sub>5</sub>) (**2b**), the *RS,SR* diastereomer of which has been crystallographically characterized.<sup>8b</sup> Note that the alkoxide carbon in **2b** bears large (C<sub>6</sub>H<sub>5</sub>), medium (CH<sub>3</sub>), and small (H) substituents. The crystal structure of (*RS,SR*)-**2b** shows the large phenyl substituent to be anti to the rhenium-oxygen bond, as sketched in II (Scheme III). Similar conformational preferences are found in crystal structures of related compounds.<sup>17</sup>

Thus, a 74/26 mixture of *RS,SR/RR,SS* diastereomers of **2b** was kept at 65 °C in C<sub>6</sub>D<sub>6</sub> for 9 h. A 82/18 (*RS,SR/RR,SS*)-**2b** mixture formed. Next, an identical reaction was conducted with diastereomerically pure (*RS,SR*)-**2b**. A 83/17 (*RS,SR/RR,SS*)-**2b** mixture formed. Hence, (*RS,SR*)-**2b** is more stable than (*RR,SS*)-**2b**. Importantly, if (*RR,SS*)-**2d** were to adopt a conformation similar to that of (*RS,SR*)-**2b**, the medium-sized alkoxide carbon substituent would be directed toward the cyclopentadienyl ligand as shown in III (Scheme III). This steric interaction is avoided in (*RS,SR*)-**2b**, as shown in II.

Next, consider the relative thermodynamic stabilities of alkoxide complexes **2a** established by the above epimerization data: (RSRR)-2a > (RRSS)-2a ≈ (RSSS)-2a > (RRRR)-2a. The alkoxide carbon substituents can again be classified as large, medium, and small, as exemplified in IV (Scheme III). Within each pair of *exo* and *endo* epimers (e.g., (RSSS)-2a and (RRRR)-2a), the more stable diastereomer is the one that allows the smaller hydrogen substituent to be directed toward the cyclopentadienyl ligand, as shown in V.

Scheme IV. Proposed Epimerization Mechanism



### Discussion

On the basis of the preceding observations, we propose that rhenium and carbon epimerization in alkoxide complexes **2** proceeds as sketched in Scheme IV. Each step and intermediate is analyzed in the following sections.

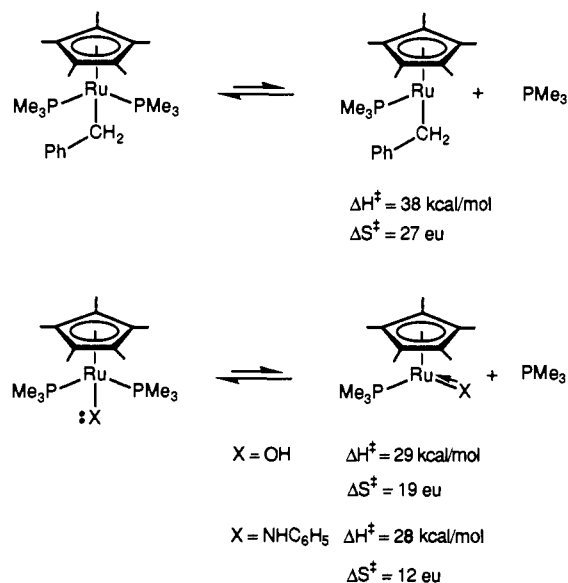
**1. Phosphine Dissociation.** Dissociative processes are often interrogated by measuring rates of formation of substitution products in the presence of excess nucleophile or ligand. Importantly, the  $k_{\text{obs}}$  for the conversion of **1** to **4** and *(RRRR)*-**2a** to **5a** (Table II) do not depend upon the  $\text{P}(p\text{-tol})_3$  concentrations, ruling out *associative* substitutions. However, the  $\Delta S^\ddagger$  ( $-7$  and  $+8$  eu) derived from the Eyring plots (Figure 2) are unusually low for dissociative processes.

In this context, Brynzda and Bercaw have similarly obtained activation parameters for  $\text{PMe}_3$  ligand dissociation from ruthenium(II) complexes of the type  $(\eta^5\text{-C}_5\text{Me}_5)\text{Ru}(\text{PMe}_3)_2(\text{X})$ ,<sup>18</sup> which can be considered "isoelectronic" with **1**. A small portion of their data is summarized in Scheme V. Dissociation is most rapid when X are amido and hydroxy ligands—superior  $\pi$  donors that have lone pairs on the ligating atoms. Furthermore, the corresponding  $\Delta S^\ddagger$  are significantly less positive than those obtained for analogous alkyl complexes. Thus, anchimeric assistance of the amido and hydroxy ligand lone pairs, which would provide a bond-making contribution to the transition state, was proposed.<sup>19</sup>

We have previously found  $\Delta S^\ddagger$  of 6–11 eu for  $\text{PPh}_3$  dissociation from the amido complex  $(\eta^5\text{-C}_5\text{H}_5)\text{Re}(\text{NO})(\text{PPh}_3)(\text{NHCH}(\text{CH}_3)\text{C}_6\text{H}_5)$ .<sup>13</sup> In view of the trends in Scheme V, we had expected slightly more positive  $\Delta S^\ddagger$  for alkoxide complexes **1** and *(RRRR)*-**2a**. It is well known that  $\Delta S^\ddagger$  values are subject to considerable experimental error.<sup>15</sup> However, replicate rate measurements were made for **1** at the extremes of Figure 2. Thus, we suggest that *both* alkoxide oxygen lone pairs provide anchimeric assistance to  $\text{PPh}_3$  ligand dissociation in **1** and **2**. Also, the crystal structure of *(RS,SR)*-**2b** (Scheme III) exhibits marked distortions from idealized octahedral geometry at rhenium, which may reflect some incipient  $\pi$  donation from the alkoxide oxygen in the ground state.<sup>8b</sup>

**2. The Alkoxide Intermediate  $(\eta^5\text{-C}_5\text{H}_5)\text{Re}(\text{NO})(\text{OR})$  (**7**).** The  $\text{PPh}_3$  dissociation product **7** (Scheme IV) can in principle adopt either a pyramidal or trigonal-planar geometry at rhenium. If **7** were pyramidal and of sufficient configurational stability, it should be possible to observe phosphine ligand exchange with

Scheme V. Previously Reported Activation Parameters for Phosphine Ligand Dissociation



*retention* of configuration at rhenium. Indeed, Brunner has reported several chiral cyclopentadienylmanganese complexes that undergo dissociative phosphine substitution with retention of configuration.<sup>20</sup>

However, the alkoxide complex *(RRRR)*-**2a** undergoes phosphine substitution with considerable *loss* of configuration at rhenium, as shown in Scheme II. Importantly, the product diastereomer ratios (*(RRRR)*/*(SRRR)*-**5a**) are independent of  $\text{P}(p\text{-tol})_3$  concentration. If **7** were pyramidal but undergoing rapid inversion, the degree of retention should increase with  $\text{P}(p\text{-tol})_3$  concentration. Also, Tilley has isolated the coordinatively unsaturated ruthenium complex  $(\eta^5\text{-C}_5\text{Me}_5)\text{Ru}(\text{P}(i\text{-Pr})_3)(\text{Cl})$ ,<sup>21</sup> which can be viewed as a model for the intermediates in Scheme V. He finds a nearly planar geometry at ruthenium, and a short Ru–Cl distance suggestive of multiple bonding. Thus, we favor a similar ground-state structure for **7**.<sup>22</sup>

However, a trigonal-planar **7** is still chiral by virtue of the alkoxide-based stereocenters. Thus, the transition states leading to substitution products *(RRRR)*/*(SRRR)*-**5a** are diastereomeric and of unequal energy. At present, we have no rationale for the preferential formation of the *less* stable diastereomer *(RRRR)*-**5a** in Scheme II.

This bias also affects the relative magnitudes of the phosphine ligand substitution and rhenium epimerization rates. For example, every  $\text{PPh}_3$  dissociation leads to substitution under the conditions of eq iv and Scheme II. If **7** exhibited no diastereoselectivity upon phosphine recombination, *half* of all  $\text{PPh}_3$  dissociations would lead to inversion of configuration at rhenium. However, on the basis of the data in Scheme II, one would expect that **7** derived from *(RRRR)*-**2a** would have a slight preference for returning to *(RRRR)*-**2a**. Accordingly, the rhenium epimerization rate of *(RRRR)*-**2a** is 36–40% of the  $\text{PPh}_3$  ligand substitution rate.

**3.  $\beta$ -Hydride Elimination.** The preceding analysis establishes that  $\text{PPh}_3$  dissociation is rate determining for epimerization at rhenium. However, since epimerization at carbon is slower, subsequent steps must be rate determining. At least one of these must involve cleavage of a bond to the alkoxide carbon. There is abundant precedent for  $\beta$ -hydride elimination in alkoxide complexes, although in most cases concomitant extrusion of an

(20) Brunner, H. *Adv. Organomet. Chem.* **1980**, *18*, 152.

(21) Campion, B. K.; Heyn, R. H.; Tilley, T. D. *J. Chem. Soc. Chem. Commun.* **1988**, 278.

(22) A reviewer has raised the interesting possibility of an agostic hydrogen ligand (as opposed to a three-electron-donor oxygen) in **7**. We suggest that the *initial* formation of **7** as formulated in Scheme IV is more likely (consistent with  $k_H/k_D = 1$  for epimerization at rhenium). However, an agostic intermediate would be very plausible on the reaction coordinate that connects **7** and **8**.

(18) Brynzda, H. E.; Domaille, P. J.; Paciello, R. A.; Bercaw, J. E. *Organometallics* **1989**, *8*, 379.

(19) For additional dissociative substitution reactions that exhibit low  $\Delta S^\ddagger$ , see: (a) Martin, G. C.; Boncella, J. M.; Wucherer, E. J. *Organometallics* **1991**, *10*, 2804. (b) Freeman, J. W.; Hallinan, N. C.; Arif, A. M.; Gedridge, R. W.; Ernst, R. D.; Basolo, F. *J. Am. Chem. Soc.* **1991**, *113*, 6509.

aldehyde or ketone appears to occur.<sup>23</sup>

Thus, we propose that 7 partitions between a return to 2 and  $\beta$ -hydride elimination to give the coordinatively saturated ketone hydride complex  $(\eta^5\text{-C}_5\text{H}_5)\text{Re}(\text{NO})(\text{H})(\text{O}=\text{CRR}')$  (8), as shown in Scheme IV. The former should be accelerated by added  $\text{PPh}_3$ . Accordingly, carbon epimerization—but not rhenium epimerization—is inhibited by added  $\text{PPh}_3$ . Furthermore, carbon epimerization rates show a  $k_{\text{H}}/k_{\text{D}}$  of ca. 2 when the alkoxy carbon hydrogen is deuterated. Comparable kinetic isotope effects have been found for  $\beta$ -hydride elimination from metal alkyls.<sup>24</sup> We therefore propose that  $\beta$ -hydride elimination from 7 is rate determining for epimerization at carbon.

However, several alternatives deserve emphasis. Transition-metal alkoxide ligands have also been observed to transfer  $\beta$ -hydrides to other coordinated ligands.<sup>25</sup> Hence, in principle the nitrosyl or cyclopentadienyl ligands of 7 could serve as  $\beta$ -hydride acceptors. However, the resulting ketone complexes would be coordinatively unsaturated, and thus likely higher in energy than 8.

The pentamethylcyclopentadienyl catalyst 1-Me<sub>5</sub> undoubtedly operates via a series of intermediates analogous to those in Scheme IV. However, although 1-Me<sub>5</sub> undergoes much more rapid  $\text{PPh}_3$  ligand dissociation than 1, it is only 2–4 times more active. Two factors are likely responsible for the enhanced dissociation rate: (1) the pentamethylcyclopentadienyl ligand is more electron releasing,<sup>26</sup> which should stabilize the electron-deficient intermediate 7-Me<sub>5</sub> relative to 7; (2) the greater steric congestion in 1-Me<sub>5</sub> (and 2-Me<sub>5</sub>) should accelerate most processes that result in a lower coordination number. However, for the same reasons, any  $\beta$ -hydride elimination of the less electrophilic, three-coordinate 7-Me<sub>5</sub> should be retarded. Hence, the net result is only a moderately more active catalyst.

**4. The Ketone Intermediate  $(\eta^5\text{-C}_5\text{H}_5)\text{Re}(\text{NO})(\text{H})(\text{O}=\text{CRR}')$  (8).** In theory, the ketone ligand in 8 might adopt either  $\sigma$  or  $\pi$  coordination modes. Both have been observed with the rhenium fragment  $[(\eta^5\text{-C}_5\text{H}_5)\text{Re}(\text{NO})(\text{PPh}_3)]^+$ .<sup>8</sup> However, the interconversion of  $\sigma$  and  $\pi$  isomers is generally rapid.<sup>27</sup> Regardless of the coordination mode, the C=O carbon remains a formal stereocenter, and R and R' must be exchanged to randomize configuration.

Our data exclude any significant amount of ketone dissociation during the epimerization process. Thus, R and R' must exchange by an *intramolecular* pathway. Importantly,  $\sigma$ -ketone complexes have been previously shown to undergo an extremely rapid intramolecular exchange of *cis/trans* C=O substituents ( $\Delta G^\ddagger = 6\text{--}7$  kcal/mol).<sup>8b,28–30</sup> This potentially complex reaction coordinate has been analyzed in detail elsewhere.<sup>8b</sup>

Thus, we propose an analogous process,  $8 \rightleftharpoons 8'$ , in Scheme IV. Reversal of  $\beta$ -hydride elimination and  $\text{PPh}_3$  dissociation then consummates the carbon epimerization reaction coordinate. In principle, inversion of configuration of 8 at rhenium could initiate other pathways for the exchange of R and R'. However, we see

no reason to invoke these less precedented and more complex alternatives.

**5. Other Epimerization Catalysts.** To our knowledge, 1 and 1-Me<sub>5</sub> rank among the most active presently available alcohol epimerization catalysts. For reference, in historically important conformational studies, Eliel equilibrated a variety of diastereomeric alcohols via two recipes: (1) nearly stoichiometric amounts of  $\text{Al}(\text{O-}i\text{Pr})_3$  in isopropyl alcohol containing a small amount of acetone at 80–90 °C; (2) similar quantities of Raney nickel in hydrocarbon or ether solvents at 56–150 °C.<sup>4</sup> Given the primary focus of this work, no attempts were made to optimize turnover numbers.

More recently, Caubère has found that complex reducing agents derived from NaH, alkoxides  $\text{RONa}$ , and transition-metal halides  $\text{MX}_n$  epimerize a variety of alcohols in THF at 63 °C.<sup>3a,b</sup> However, stoichiometric quantities of metal halides were commonly employed. Nugent has reported that Zr(IV) and Ta(V) alkoxides catalyze the racemization of 2-butanol at 200 °C.<sup>3c</sup> A palladium-based epimerization catalyst has also been described.<sup>3d</sup>

Eliel has further shown that equilibrium constants for diastereomeric alcohols can differ in hydrocarbon and protic solvents due to hydrogen bonding.<sup>4d</sup> The final alcohol ratios given for 1-Me<sub>5</sub> in Table I compare closely with literature data obtained in benzene or toluene.<sup>31,32</sup> We speculate that the slightly lower alcohol ratios sometimes obtained with 1 might be due to competing deactivation processes. For example, a byproduct is evident in Figure 1. Also, the small amounts of  $\text{PPh}_3$  noted in some epimerizations could be due to the formation of *bridging* alkoxide complexes  $[(\eta^5\text{-C}_5\text{H}_5)\text{Re}(\text{NO})(\mu\text{-OR})]_2$ , which are formal dimers of 7. Related dimers readily form from the corresponding amido complexes.<sup>14</sup> However, such equilibria should not be as favorable for pentamethylcyclopentadienyl analogues. Also, any dimers would not necessarily be catalytically inactive; rather, generation of the key intermediate 7 would simply require higher temperature.

Nearly all alcohol epimerization catalysts described to date appear to involve  $\beta$ -hydride elimination from metal alkoxide intermediates. Since this is a common elementary step,<sup>24</sup> there is no obvious reason why a variety of metal alkoxide complexes should not be effective epimerization catalysts. However, to our knowledge, 1 and 1-Me<sub>5</sub> are the first well-defined homogeneous catalysts involving a transition metal in a low oxidation state. Alkoxide complexes that are coordinatively unsaturated, and/or undergo particularly rapid  $\beta$ -hydride eliminations, may prove to be more reactive than 1 and 1-Me<sub>5</sub>.

**6. Summary.** Methoxide complexes  $(\eta^5\text{-C}_5\text{R}_5)\text{Re}(\text{NO})(\text{PPh}_3)(\text{OCH}_3)$  constitute a new generation of alcohol epimerization catalysts. Diastereomeric secondary alkoxide complexes initially form, which undergo facile  $\text{PPh}_3$  dissociation and sequential epimerization at rhenium and carbon. A conformational model that rationalizes diastereomer stabilities—a “chiral recognition” phenomenon—has been developed. The carbon epimerization step involves  $\beta$ -hydride elimination, and the possibility of coupling further transformations (e.g., involving remote functionality) into this carbon–hydrogen bond activation process should not be overlooked.

## Experimental Section

**General Methods.** General procedures have been recently described.<sup>8b</sup> All NMR spectra were recorded on Varian XL-300 spectrometers, and referenced to internal  $\text{Si}(\text{CH}_3)_4$  (<sup>1</sup>H, <sup>13</sup>C) or external 85%  $\text{H}_3\text{PO}_4$  (<sup>31</sup>P). GC analyses were conducted on a Hewlett-Packard 5890 chromatograph (25-m  $\times$  0.2-mm Carbowax column). Mass spectra were obtained on a Finnigan MAT-95 instrument with a VG data system 2000.

Solvents and reagents were purified as follows: benzene and hexane, distilled from Na/benzophenone;  $\text{CH}_2\text{Cl}_2$ , distilled from  $\text{P}_2\text{O}_5$ ;  $\text{CH}_3\text{OH}$

(23) Selected examples: (a) Bryndza, H. E.; Calabrese, J. C.; Marsi, M.; Roe, D. C.; Tam, W.; Bercaw, J. E. *J. Am. Chem. Soc.* **1986**, *108*, 4805. (b) Hoffman, D. M.; Lappas, D.; Wierda, D. A. *J. Am. Chem. Soc.* **1989**, *111*, 1531. (c) Kölle, U.; Kang, B.-S.; Raabe, G.; Krüger, C. *J. Organomet. Chem.* **1990**, *386*, 261.

(24) (a) Li, M.-Y.; San Filippo, J., Jr. *Organometallics* **1983**, *2*, 554. (b) Whitesides, G. M.; Gaasch, J. F.; Stedronsky, E. R. *J. Am. Chem. Soc.* **1972**, *94*, 5258; see ref 36.

(25) Selected examples: (a) Ishii, Y.; Nakano, T.; Inada, A.; Kishigami, Y.; Sakurai, K.; Ogawa, M. *J. Org. Chem.* **1986**, *51*, 240. (b) Schröder, D.; Schwarz, H. *Angew. Chem., Int. Ed. Engl.* **1990**, *29*, 910. (c) Strickler, J. R.; Bruck, M. A.; Wexler, P. A.; Wigley, D. E. *Organometallics* **1990**, *9*, 266.

(26) (a) Sowa, J. R., Jr.; Angelici, R. J. *J. Am. Chem. Soc.* **1991**, *113*, 2537. (b) Choi, M.-G.; Angelici, R. J. *Ibid.* **1991**, *113*, 5651.

(27) (a) Quirós Méndez, N.; Arif, A. M.; Gladysz, J. A. *Angew. Chem., Int. Ed. Engl.* **1990**, *29*, 1473. (b) Quirós Méndez, N.; Mayne, C. L.; Gladysz, J. A. *Ibid.* **1990**, *29*, 1475.

(28) Dalton, D. M.; Gladysz, J. A. *J. Chem. Soc., Dalton Trans.* **1991**, 2741.

(29) (a) Courtot, P.; Pichon, R.; Salaün, J.-Y. *J. Organomet. Chem.* **1985**, *286*, C17. (b) Auffret, J.; Courtot, P.; Pichon, R.; Salaün, J.-Y. *J. Chem. Soc., Dalton Trans.* **1987**, 1687.

(30) Faller, J. W.; Ma, Y. *J. Am. Chem. Soc.* **1991**, *113*, 1579.

(31) *exo/endo*-Borneol, 29/71 (Na/fluorenone, toluene, ca. 110 °C); *endo/exo*-norborneol, 20/80 (Na/fluorenone, toluene, ca. 110 °C); *cis/trans*-2-methylcyclohexanol, 23/77 (Raney nickel, benzene, ca. 80 °C); *cis/trans*-4-methylcyclohexanol, 30/70 (Raney nickel, benzene, ca. 80 °C).<sup>4e</sup>

(32) To our knowledge, equilibrium constants for  $\alpha/\beta$ -cholestanol are not available in aprotic solvents. Other data 16/84 ( $\text{Al}(\text{OR})_3/\text{ROH}/\text{cyclohexanone}$ , ca. 100 °C): Nace, H. R.; O'Connor, G. L. *J. Am. Chem. Soc.* **1951**, *73*, 5824.

(EM Science), purged with  $N_2$ ; pentane, distilled from  $LiAlH_4$ ;  $C_6D_6$  and  $C_6D_5CD_3$  (Cambridge Isotopes),  $P(p\text{-tol})_3$  (Strem),  $p\text{-CH}_3C_6H_4SO_3H \cdot H_2O$ ,  $NaOCH_3$ ,  $HBf_4 \cdot OEt_2$ ,  $Et_3N$ , *cis*-2-methylcyclohexanol, *cis*-4-methylcyclohexanol, (-)-*endo*-borneol (Aldrich), and (+)-*endo*-borneol (Fluka), used as received; ( $\pm$ )-*exo*-borneol and ( $\pm$ )-*endo*-borneol (Aldrich), crystallized from pentane; (+)-*exo*-borneol,<sup>33</sup> (-)-*exo*-borneol,<sup>33</sup> and camphor-3-*exo*- $d_1$ ,<sup>34</sup> prepared by literature methods; (+)- $\alpha$ -cholestanol, prepared by  $Li(s\text{-}C_4H_9)_3BH$  reduction<sup>35</sup> of (+)-cholestanone and purified by a literature method.<sup>32</sup> Florisil was treated with concentrated  $NH_4OH$  (30% v/w).

( $\eta^5\text{-}C_5Me_5$ ) $Re(NO)(PPh_3)(OCH_3)(1\text{-}Me_5)$ . A Schlenk flask was charged with ( $\eta^5\text{-}C_5Me_5$ ) $Re(NO)(PPh_3)(CH_3)$  (660.2 mg, 1.050 mmol),<sup>7</sup>  $p\text{-CH}_3C_6H_4SO_3H \cdot H_2O$  (598.0 mg, 3.144 mmol),  $CH_3OH$  (200 mL), and a stir bar. The solution was stirred and turned deep orange. After 15 min, a  $NaOCH_3/HOCH_3$  solution (4.37 M; 2.9 mL, 12.6 mmol) was added. After 4 h, solvent was removed in vacuo. The resulting orange solid was extracted with benzene (ca. 50 mL). The extract was filtered under  $N_2$  through florisil in a Kramer filter,<sup>35</sup> and the orange band was eluted with additional benzene (50 mL). The eluate was concentrated to ca. 20 mL, and hexane was added (50 mL). The resulting orange precipitate was collected by filtration and dried in vacuo to give **1-Me<sub>5</sub>** (346.0 mg, 0.537 mmol, 51%), mp 164–165 °C dec. Anal. Calcd for  $C_{29}H_{33}NO_2PR_2$ : C, 54.02; H, 5.16. Found: C, 53.88; H, 5.17. IR ( $cm^{-1}$ , KBr):  $\nu_{NO}$  1613 (vs).  $^1H$  NMR ( $\delta$ ,  $C_6D_6$ ): 7.80–7.74 (m, 6 H of 3 Ph), 7.16–6.97 (m, 9 H of 3 Ph), 4.25 (s, OMe), 1.60 (s, 5 CMe).  $^{13}C\{^1H\}$  NMR (ppm,  $C_6D_6$ ): 135.1 (*i*-Ph),<sup>36</sup> 134.4 (d,  $J_{CP}$  = 9.6 Hz, *o*-Ph), 129.6 (s, *p*-Ph), 128.0 (d,  $J_{CP}$  = 9.6 Hz, *m*-Ph), 99.7 (s,  $C_5Me_5$ ), 71.4 (d,  $J_{CP}$  = 6.0 Hz, OMe), 10.5 (s,  $C_5Me_5$ ).  $^{31}P\{^1H\}$  NMR (ppm,  $C_6D_6$ ): 16.6 (s).

( $\eta^5\text{-}C_5H_5$ ) $Re(NO)(P(p\text{-tol})_3)(OCH_3)(4)$ . The methyl complex ( $\eta^5\text{-}C_5H_5$ ) $Re(NO)(P(p\text{-tol})_3)(CH_3)$  (651.6 mg, 1.085 mmol),<sup>14</sup>  $p\text{-CH}_3C_6H_4SO_3H \cdot H_2O$  (619.2 mg, 3.255 mmol),  $CH_3OH$  (100 mL), and  $NaOCH_3/HOCH_3$  (4.37 M; 2.9 mL, 12.6 mmol) were combined in a procedure analogous to that given for **1-Me<sub>5</sub>**. A similar workup gave **4** as an orange powder (285.0 mg, 0.462 mmol, 43%), mp 195 °C dec. Anal. Calcd for  $C_{27}H_{29}NO_2PR_2$ : C, 52.58; H, 4.74. Found: C, 52.65; H, 4.72. IR ( $cm^{-1}$ , KBr):  $\nu_{NO}$  1613 (vs).  $^1H$  NMR ( $\delta$ ,  $C_6D_6$ ): 7.75–7.69 (m, 6 H of 3 Ph), 6.95–6.92 (m, 6 H of 3 Ph), 4.96 (s,  $C_5H_5$ ), 4.40 (s, OMe), 1.98 (s, 3CMe).  $^{13}C\{^1H\}$  NMR (ppm,  $C_6D_6$ ): 140.1 (s, *p*-Ph), 134.4 (d,  $J_{CP}$  = 10.6 Hz, *o*-Ph), 132.9 (d,  $J_{CP}$  = 52.6 Hz, *i*-Ph), 129.2 (d,  $J_{CP}$  = 10.1 Hz, *m*-Ph), 90.6 (d,  $J_{CP}$  = 15.8 Hz,  $C_5H_5$ ), 75.8 (d,  $J_{CP}$  = 6.7 Hz, OMe), 21.1 (d,  $J_{CP}$  = 10.4 Hz, 3 CMe).  $^{31}P\{^1H\}$  NMR (ppm,  $C_6D_6$ ): 14.4 (s).

(*RSSS*)-( $\eta^5\text{-}C_5H_5$ ) $Re(NO)(PPh_3)(OC_{10}H_{17})$  (*RSSS*-**2a**). A Schlenk flask was charged with (+)-(*S*)-( $\eta^5\text{-}C_5H_5$ ) $Re(NO)(PPh_3)(CH_3)$  ((+)-*S*)-**9**)<sup>10</sup> (250.0 mg, 0.448 mmol),  $CH_2Cl_2$  (5 mL), and a stir bar, and cooled to -80 °C. Then  $HBf_4 \cdot OEt_2$  (0.065 mL, 0.52 mmol) was added with stirring to generate (*S*)-[( $\eta^5\text{-}C_5H_5$ ) $Re(NO)(PPh_3)(C(CH_2Cl)_2)]^+BF_4^-$ .<sup>11</sup> After 5 min, a solution of (+)-*exo*-borneol (140.5 mg, 0.911 mmol) in  $CH_2Cl_2$  (2 mL) was added. The cooling bath was allowed to slowly warm to -20 °C, and then replaced with an ice bath. The volatiles were removed under oil pump vacuum. The flask was cooled again to -80 °C, and  $CH_2Cl_2$  (5 mL) and  $Et_3N$  (0.085 mL, 0.59 mmol) were added with stirring. After 5 min, the flask was transferred to an ice bath. After 15 min, the volatiles were removed under oil pump vacuum, and the orange residue was extracted with benzene. The extract was filtered under  $N_2$  through florisil in a Kramer filter.<sup>35</sup> The receiving flask was placed in an ice bath to avoid product epimerization, and hexane was added to prevent freezing. Solvent was removed in vacuo to give (*RSSS*)-**2a** as an orange powder (85.0 mg, 0.122 mmol, 27%). Some (+)-*exo*-borneol was detected by  $^1H$  and  $^{13}C$  NMR, and thus correct microanalyses were not obtained. IR ( $cm^{-1}$ , KBr):  $\nu_{NO}$  1626 (vs).  $^1H$  NMR ( $\delta$ ,  $C_6D_5CD_3$ , 0 °C): 7.73–7.58 (m, 6 H of 3 Ph), 7.16–7.00 (m, 9 H of 3 Ph), 4.82 (s,  $C_5H_5$ ), 3.62 (m, OCH), 0.92 (s, Me), 0.85 (s, Me), 0.54 (s, Me).<sup>37</sup>  $^{13}C\{^1H\}$  NMR (ppm,  $C_6D_5CD_3$ , 0 °C): 136.3 (d,  $J_{CP}$  = 50.4 Hz, *i*-Ph), 134.2 (d,  $J_{CP}$  = 10.4 Hz, *o*-Ph), 130.0 (s, *p*-Ph), 128.2 (d,  $J_{CP}$  = 10.2 Hz, *m*-Ph), 103.8 (d,  $J_{CP}$  = 5.3 Hz, OCH), 91.1 (s,  $C_5H_5$ ), 51.2 (s, 46.2 (s), 45.6 (s), 43.8 (s), 35.4 (s), 28.3 (s), 21.2 (s,  $CH_3$ ), 20.2 (s,  $CH_3$ ), 13.1 (s,  $CH_3$ ).  $^{31}P\{^1H\}$  NMR (ppm,  $C_6D_5CD_3$ , 0 °C): 16.0 (s).

(*RRRR*)-**2a**. Complex (+)-(*S*)-**9** (249.5 mg, 0.447 mmol),  $CH_2Cl_2$  (5 mL),  $HBf_4 \cdot OEt_2$  (0.065 mL, 0.52 mmol), (-)-*exo*-borneol (138.4 mg, 0.897 mmol), and  $Et_3N$  (0.085 mL, 0.59 mmol) were combined in a

procedure analogous to that given for (*RSSS*)-**2a**. A similar workup gave (*RRRR*)-**2a** as an orange powder, which was dried in vacuo (73.0 mg, 0.105 mmol, 23%), mp 138–140 °C dec. Anal. Calcd for  $C_{33}H_{37}NO_2PR_2$ : C, 56.88; H, 5.35. Found: C, 56.11; H, 5.38. IR ( $cm^{-1}$ , KBr):  $\nu_{NO}$  1636 (vs).  $^1H$  NMR ( $\delta$ ,  $C_6D_5CD_3$ , 0 °C): 7.74–7.57 (m, 6 H of 3 Ph), 7.10–6.97 (m, 9 H of 3 Ph), 4.85 (s,  $C_5H_5$ ), 3.99 (m, OCH), 1.03 (s, Me), 0.84 (s, Me), 0.80 (s, Me).<sup>37</sup>  $^{13}C\{^1H\}$  NMR (ppm,  $C_6D_5CD_3$ , 0 °C): 135.9 (d,  $J_{CP}$  = 50.3 Hz, *i*-Ph), 134.3 (d,  $J_{CP}$  = 10.4 Hz, *o*-Ph), 130.0 (s, *p*-Ph), 128.2 (d,  $J_{CP}$  = 10.2 Hz, *m*-Ph), 104.7 (d,  $J_{CP}$  = 5.7 Hz, OCH), 90.6 (s,  $C_5H_5$ ), 50.8 (s), 46.4 (s), 45.7 (s), 44.1 (s), 35.2 (s), 28.2 (s), 21.1 (s,  $CH_3$ ), 20.7 (s,  $CH_3$ ), 13.0 (s,  $CH_3$ ).  $^{31}P\{^1H\}$  NMR (ppm,  $C_6D_5CD_3$ , 0 °C): 17.2 (s).

(*RRSS*)-**2a**. Complex (+)-(*S*)-**9** (250.0 mg, 0.448 mmol),  $CH_2Cl_2$  (5 mL),  $HBf_4 \cdot OEt_2$  (0.065 mL, 0.52 mmol), (-)-*endo*-borneol (139.7 mg, 0.906 mmol), and  $Et_3N$  (0.085 mL, 0.59 mmol) were combined in a procedure analogous to that given for (*RSSS*)-**2a**. A similar workup gave (*RRSS*)-**2a** as an orange powder, which was dried in vacuo (118.0 mg, 0.169 mmol, 38%). Some (-)-*endo*-borneol was detected by  $^1H$  and  $^{13}C$  NMR, and thus correct microanalyses were not obtained. IR ( $cm^{-1}$ , KBr):  $\nu_{NO}$  1628 (vs).  $^1H$  NMR ( $\delta$ ,  $C_6D_6$ ) 7.78–7.66 (m, 6 H of 3 Ph), 7.13–6.98 (m, 9 H of 3 Ph), 4.87 (s,  $C_5H_5$ ), 4.23 (m, OCH), 1.25 (s, Me), 0.99 (s, Me), 0.90 (s, Me).<sup>37</sup>  $^{13}C\{^1H\}$  NMR (ppm,  $C_6D_6$ ): 136.0 (d,  $J_{CP}$  = 49.1 Hz, *i*-Ph), 134.5 (d,  $J_{CP}$  = 9.8 Hz, *o*-Ph), 130.2 (s, *p*-Ph), 128.4 (d,  $J_{CP}$  = 9.5 Hz, *m*-Ph), 102.4 (d,  $J_{CP}$  = 5.5 Hz, OCH), 90.8 (s,  $C_5H_5$ ), 51.2 (s), 48.2 (s), 46.1 (s), 42.3 (s), 29.9 (s), 26.9 (s), 21.1 (s,  $CH_3$ ), 19.9 (s,  $CH_3$ ), 15.1 (s,  $CH_3$ ).  $^{31}P\{^1H\}$  NMR (ppm,  $C_6D_6$ ): 16.6 (s).

(*RSRR*)-**2a**. Complex (+)-(*S*)-**9** (249.5 mg, 0.447 mmol),  $CH_2Cl_2$  (5 mL),  $HBf_4 \cdot OEt_2$  (0.065 mL, 0.52 mmol), (+)-*endo*-borneol (137.8 mg, 0.893 mmol), and  $Et_3N$  (0.085 mL, 0.59 mmol) were combined in a procedure analogous to that given for (*RSSS*)-**2a**. A similar workup gave (*RSRR*)-**2a** as an orange powder, which was dried in vacuo (152.0 mg, 0.218 mmol, 49%), mp 145–147 °C dec. Anal. Calcd for  $C_{33}H_{37}NO_2PR_2$ : C, 56.88; H, 5.35. Found: C, 56.74; H, 5.38. IR ( $cm^{-1}$ , KBr):  $\nu_{NO}$  1616 (vs).  $^1H$  NMR ( $\delta$ ,  $C_6D_6$ ): 7.80–7.62 (m, 6 H of 3 Ph), 7.11–6.91 (m, 9 H of 3 Ph), 4.85 (s,  $C_5H_5$ ), 3.84 (m, OCH), 1.05 (s, Me), 0.92 (s, 2Me).<sup>37</sup>  $^{13}C\{^1H\}$  NMR (ppm,  $C_6D_6$ ): 136.1 (d,  $J_{CP}$  = 50.4 Hz, *i*-Ph), 134.5 (d,  $J_{CP}$  = 10.6 Hz, *o*-Ph), 130.2 (d,  $J_{CP}$  = 2.2 Hz, *p*-Ph), 128.4 (d,  $J_{CP}$  = 10.1 Hz, *m*-Ph), 99.3 (d,  $J_{CP}$  = 6.1 Hz, OCH), 90.9 (d,  $J_{CP}$  = 2.1 Hz,  $C_5H_5$ ), 51.6 (s), 48.1 (s), 45.8 (s), 41.1 (s), 28.9 (s), 27.2 (s), 20.9 (s,  $CH_3$ ), 19.5 (s,  $CH_3$ ), 14.8 (s,  $CH_3$ ).  $^{31}P\{^1H\}$  NMR (ppm,  $C_6D_6$ ): 16.8 (s).

**Standard Procedures for NMR Rate Experiments.** For rates measured by  $^1H$  NMR, probe temperatures were calibrated with ethylene glycol (estimated error  $\pm 1$  °C).<sup>38</sup> For rates measured by  $^{31}P\{^1H\}$  NMR, a sealed capillary of ethylene glycol was inserted into a sample. After an equilibration period (to allow for decoupler-induced heating), the observed nucleus was switched to  $^1H$  and the temperature immediately calibrated as above. Corrections averaged 2 °C. Probe temperatures were equilibrated to the temperature of a rate experiment prior to sample introduction. Samples were allowed to equilibrate for 7 min (while magnet homogeneity was adjusted) prior to rate data acquisition.

**Alcohol Epimerizations.** The following procedures are representative, and additional data are given in the supplementary material. (A) A 5-mm NMR tube was charged with **1** (9.6 mg, 0.017 mmol) and ( $\pm$ )-*exo*-borneol (26.3 mg, 0.170 mmol), and capped with a septum. A  $N_2$  atmosphere was established, and  $C_6D_6$  (0.6 mL) was added. The tube was transferred to a 65 °C NMR probe, and rate data were acquired (10 spectra/5 h) as described above. The *endo/exo*-borneol ratios were assayed by integration of the *CHOH*  $^1H$  NMR resonances ( $\delta$  3.84 (m) and 3.40 (m)). The tube was transferred to a 65 °C oil bath, and checked by NMR every 24 h until the normalized *endo/exo* ratio changed by less than  $\pm 2$ . (B) A 5-mm NMR tube was charged with **1** (11.3 mg, 0.020 mmol), ( $\pm$ )-*exo*-borneol (30.5 mg, 0.198 mmol), and  $C_6D_6$  (0.6 mL) as in the preceding experiment, and placed in a 65 °C oil bath. After 48 h, the *endo/exo* ratio was assayed by  $^1H$  NMR (68/32). Tetradecane (14.4 mg, 0.073 mmol) standard was added, and capillary GC analysis (80–150 °C, 5 °C/min) showed *exo*-borneol (0.065 mmol, 33%), *endo*-borneol (0.120 mmol, 62%), and camphor (0.010 mmol, 5%).

**Rate of Epimerization of **2a**.** The following procedure is representative. A 5-mm NMR tube was charged with (*RRRR*)-**2a** (15.7 mg, 0.023 mmol) and capped with a septum. A  $N_2$  atmosphere was established, and  $C_6D_6$  (0.6 mL) was added. The tube was transferred to a NMR probe, and rate data were acquired as described above. The (*RRRR*)/(*SRRR*)-**2a** ratios were assayed by integration of the  $^{31}P$  NMR resonances (17.1 and 15.9 ppm, 40 °C). Standard procedures gave the data in Table III.<sup>9</sup>

(33) Brown, H. C.; Krishnamurthy, S. *J. Am. Chem. Soc.* **1972**, *94*, 7159.

(34) Joshi, G. C.; Warnhoff, E. W. *J. Org. Chem.* **1972**, *37*, 2383.

(35) Brown, H. C. *Organic Syntheses via Boranes*; Wiley: New York, 1975; Figure 9.26. Aldrich Catalog No. Z10,139-7.

(36) One line of the doublet is obscured.

(37) Only selected alkoxide ligand  $^1H$  NMR resonances are given.

(38) Van Geet, A. L. *Anal. Chem.* **1968**, *40*, 2227.



**Rate of Reaction of 1 and P(*p*-tol)<sub>3</sub>.** The following procedure is representative. A 5-mm NMR tube was charged with 1 (16.0 mg, 0.028 mmol) and P(*p*-tol)<sub>3</sub> (170.0 mg, 0.559 mmol) and capped with a septum. A N<sub>2</sub> atmosphere was established, and C<sub>6</sub>D<sub>6</sub> (0.7 mL) was added. The tube was transferred to a NMR probe, and rate data were acquired as described above. The concentrations of 1 and 4 were assayed by integration of the <sup>31</sup>P NMR resonances (17.2 and 14.4 ppm, 39 °C). The data are presented in Table II.

**Rate of Reaction of (RRRR)-2a and P(*p*-tol)<sub>3</sub>.** The following procedure is representative. A 5-mm NMR tube was charged with (RRRR)-2a (16.3 mg, 0.023 mmol), P(*p*-tol)<sub>3</sub> (72.0 mg, 0.239 mmol), and C<sub>6</sub>D<sub>6</sub> (0.7 mL) in a manner analogous to the preceding experiment. The tube was transferred to a NMR probe, and rate data were acquired

as described above. Concentrations of (RRRR)-2a and (RRRR)/(SRRR)-(η<sup>5</sup>-C<sub>5</sub>H<sub>5</sub>)Re(NO)(P(*p*-tol)<sub>3</sub>)(OC<sub>10</sub>H<sub>17</sub>) (5a) were assayed by integration of the <sup>31</sup>P NMR resonances (17.2, 13.2, and 14.2 ppm, 29 °C). The data are presented in Table II.

**Acknowledgment.** We thank the DOE for support of this research, Dr. C. M. Garner for preliminary observations, and the Ministry of Education and Science of Spain and the Fulbright Commission for a postdoctoral fellowship (I.S.L.).

**Supplementary Material Available:** Details of additional experiments (2 pages). Ordering information is given on any current masthead page.

## Electrostatic Micellar Effects on the Rate of Spontaneous Decomposition of *m*-Nitrophenyl 9-Fluorene-carboxylate

Valdir R. Correia,<sup>†</sup> Iolanda Midea Cuccovia, Magaly Stelmo, and Hernan Chaimovich\*

Contribution from the Departamento de Bioquímica, Instituto de Química da Universidade de São Paulo, Caixa Postal 20780, São Paulo, SP, CEP 01498, Brazil.

Received December 17, 1990. Revised Manuscript Received October 23, 1991

**Abstract:** The effects of neutral, ionic, and zwitterionic micelles on the rate of the spontaneous decomposition of *m*-nitrophenyl 9-fluorene-carboxylate (I) were determined. Neutral micelles of a poly(oxyethylene) detergent produce a small increase in the decomposition rate. Negatively charged micelles of sodium dodecyl sulfate catalyze the reaction 2-fold while positively charged micelles of hexadecyltrimethylammonium bromide (CTAB) inhibit by a similar factor. Micelles of *N*-hexadecyl-*N,N*-dimethylammonium 3-propanesulfonate inhibit the decomposition of I to a larger extent than those of *O*-hexadecylphosphorylcholine while lysolecithin micelles do not affect the reaction rate. Thus, charge orientation of the monomer does not determine the kinetic effects of zwitterionic micelles on the rate of decomposition of I. The rate modifications produced by micelles on this reaction are consistent with electrostatic effects on the relative energies of initial and transition states.

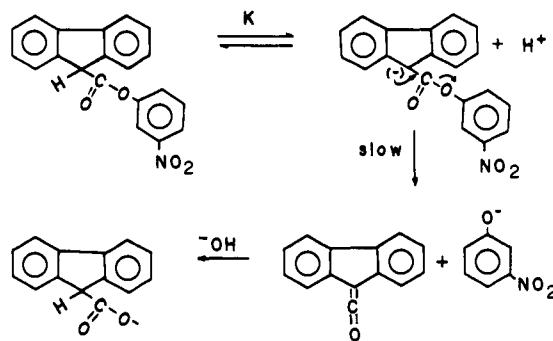
### Introduction

Micellar incorporation of a substrate decomposing spontaneously can produce major effects in the reaction rate.<sup>1</sup> For different reactions distinct features of the micellar interface have been singled out as determining the observed effect. These include (a) conformer stabilization,<sup>2</sup> (b) decrease of hydration of the nucleophile,<sup>3</sup> (c) medium effects related to local polarity,<sup>4</sup> and (d) specific interactions of ionic head groups with transition states.<sup>5</sup>

The consideration of micelles as a separate pseudophase has greatly facilitated mechanistic descriptions and quantitative rate analysis of chemical reactions in micelles.<sup>1</sup> However, the micellar reaction site is not a continuous phase.<sup>1</sup> Reactions of hydrophilic (and relatively hydrophobic) substrates occur in the micelle-water interface.<sup>1</sup> At this site the effective polarity may differ significantly from that in the bulk solvent, and the local electrostatic field in both ionic and zwitterionic micelles may be considerable.<sup>1,6,7</sup> It has been suggested that specific effects of micellar charge in rates of unimolecular reactions can only be expected when formation of the transition state involves an ionization, as is the case for hydrolysis of *tert*-butyl chloride.<sup>8</sup> A study of the effect of micelles of detergents exhibiting different charge and/or dipoles on a monomolecular reaction should contribute to a better understanding of Coulombic effects on interfacial reactions.

Here we report that the E1cB decomposition of *m*-nitrophenyl 9-fluorene-carboxylate (I) (Scheme I) is catalyzed by negatively charged micelles, unaffected by neutral micelles, and inhibited by positively charged micelles. The effects of zwitterionic micelles depend on the nature of the detergent. These effects can be

### Scheme I



accommodated with current models of micellar structure and are consistent with stabilization of the initial state by ion pairing of

(1) (a) Fendler, J. H. *Membrane Mimetic Chemistry*; Wiley-Interscience: New York, 1982. (b) Bunton, C. A.; Savelli, G. *Adv. Phys. Org. Chem.* **1986**, *22*, 231-309.

(2) (a) Oliveira, A. G.; Cuccovia, I. M.; Chaimovich, H. *J. Pharm. Sci.* **1990**, *79*, 37-42. (b) Oliveira, A. G.; Nothenberg, M. S.; Cuccovia, I. M.; Chaimovich, H. *J. Phys. Org. Chem.* **1991**, *4*, 19-24. (c) Cuccovia, I. M.; Schroter, E. H.; de Baptista, R. C.; Chaimovich, H. *J. Org. Chem.* **1977**, *42*, 3400-3403.

(3) Cerichelli, G.; Luchetti, L.; Mancini, G.; Muzzioli, M. N.; Germani, R.; Ponti, P. P.; Spreti, N.; Savelli, G.; Bunton, C. A. *J. Chem. Soc., Perkin Trans. 2* **1989**, 1081-1085.

(4) Bunton, C. A.; Minch, M. J.; Sepulveda, L.; Hidalgo, J. *J. Am. Chem. Soc.* **1973**, *95*, 3262-3272.

(5) Bunton, C. A. In *Solution Chemistry of Surfactants*; Mittal, K. L., Ed.; Plenum Press: New York, 1979; Vol. 2, pp 519-540.

(6) Handa, T.; Nakagaki, M.; Miyajima, K. *J. Colloid Interface Sci.* **1990**, *137*, 253-262.

\* To whom correspondence should be addressed.

<sup>†</sup> Present address: Departamento de Química, Universidade Federal de Santa Catarina, Florianópolis, SC.